Published in final edited form as:
J Phys Chem B. 2008 October 23; 112(42): 13263–13272. doi:10.1021/jp804640p.

Fluorescence Resonance Energy Transfer in Polydiacetylene Liposomes

Xuelian Li[†], **Shelton Matthews**[‡], and **Punit Kohli**[*,†]
Department of Chemistry and Biochemistry, Southern Illinois University, Carbondale, Illinois 62901 and Department of Chemistry, Grambling State University, Grambling, Louisiana 71245

Abstract

Conjugated polydiacetylene (PDA) possessing stimuli-responsive properties has been intensively investigated for developing efficient sensors. We report here fluorescence resonance energy transfer (FRET) in liposomes synthesized using different molar ratios of dansyl-tagged diacetylene and diacetylene–carboxylic acid monomers. Photopolymerization of diacetylene resulted in cross-linked PDA liposomes. We used steady-state electronic absorption, emission, and fluorescence anisotropy (FA) analysis to characterize the thermal-induced FRET between dansyl fluorophores (donor) and PDA (acceptor). We found that the monomer ratio of acceptor to donor (R_{ad}) and length of linkers (functional part that connects dansyl fluorophores to the diacetylene group in the monomer) strongly affected FRET. For R_{ad} = 10 000, the acceptor emission intensity was amplified by more than 18 times when the liposome solution was heated from 298 to 338 K. A decrease in R_{ad} resulted in diminished acceptor emission amplification. This was primarily attributed to lower FRET efficiency between donors and acceptors and a higher background signal. We also found that the FRET amplification of PDA emissions after heating the solution was much higher when dansyl was linked to diacetylene through longer and flexible linkers than through shorter linkers. We attributed this to insertion of dansyl in the bilayer of the liposomes, which led to an increased dansyl quantum yield and a higher interaction of multiple acceptors with limited available donors. This was not the case for shorter and more rigid linkers where PDA amplification was much smaller. The present studies aim at enhancing our understanding of FRET between fluorophores and PDA-based conjugated liposomes. Furthermore, receptor tagged onto PDA liposomes can interact with ligands present on proteins, enzymes, and cells, which will produce emission sensing signal. Therefore, using the present approach, there exist opportunities for designing FRET-based highly sensitive and selective chemical and biochemical sensors.

Introduction

Conjugated polymers have attracted a lot of attention because of their wide range of applications in the fields of molecular and ion sensing and detection, organic light emitting devices, optoelectronic, solar, and photovoltaic devices, and actuators.[1–3] Many excellent reviews on conjugated polymers for sensing applications are available in the literature.[2] In particular, sensors based on FRET between conjugated polymers and fluorophores are investigated by many groups because conjugated polymers provide signal amplification in

*To whom correspondence should be addressed. E-mail: E-mail: pkohli@chem.siu.edu.
[†]Southern Illinois University.
[‡]Grambling State University.

Supporting Information Available: The effect of polymerization time on absorbance of PDA and the effect of polarity of solvents on emission of dansyl fluorophore. Emission and FTIR spectra of PDA in blue and red phases. This material is available free of charge via the Internet at http://pubs.acs.org.

response to external stimulation.[2] Recently, Leclerc and co-workers used polythiophene and other conjugated polymers for detection of ions such as I^- and Na^+, protein, and nucleic acids.[4] Leclerc's group also demonstrated FRET between cationic polythiophene and fluorophore-tagged anionic DNA molecules for highly sensitive detection of cDNA.[4h] Similarly, the groups of Heeger and Bazan used FRET between organic fluorophores and fluorene derivative conjugative polymers for highly sensitive detection of nucleic acids and pepetides.[3a–f] Whitten's group used conjugated phenylene–vinylene polymers for reversible FRET-based highly sensitive protein sensing.[3j] PDA, which is also a conjugated polymer, has been extensively studied for decades for applications such as the sensing of ions, proteins, bacteria, and viruses, electronic transport properties in crystals, and optical properties in solution and solid phases.[5] Most of the reported PDA sensors are based on colorimetric changes such that a change in color is observed when receptors attached to PDA interact with ligands of molecules or particles to be sensed.[5] On the other hand, PDA-based FRET assay which can be more sensitive than colorimetric-based sensors are less exploited.[6]

Recently, we[6a] and others[6b–e] demonstrated FRET between PDA and organic fluorophores. Reppy and co-workers detected *E. coli* using PDA-based FRET assay.[6d] Similarly, Cheng used FRET between PDA and BODIPY fluorophores for sensing of amines in solution.[6c] We have shown that the FRET efficiency between dansyl (donor) and polydiacetylene (PDA, acceptor) can be modulated by thermal treatment of the dansyl-tagged PDA liposome solution. The increase in the FRET efficiency was partially attributed to a large increase in the spectral overlap between the emission spectrum of dansyl and the absorption spectrum of PDA (Figure 2) and to an increase in the quantum yield (Q_y) of the red form PDA after thermal treatment.[6a] A detailed systematic study of FRET between donor fluorophores and PDA acceptor is not yet reported. To further increase our understanding of FRET in the fluorophore–PDA system, we investigated the effect of different parameters such as donor concentration in the liposomes and chemical structure of the monomers on FRET efficiency. Specifically, we studied two major factors: (1) the effect of monomer ratio of acceptor to donor (R_{ad}) and (2) the effect of length and flexibility of the linkers that connect donor to acceptor. These two factors provided us with crucial information for optimization of FRET into our system. To accomplish this we synthesized three donor-tagged monomers which were incorporated in the liposomes. These monomers were synthesized to systematically study the effect of linker length (L) on FRET. We show that FRET between dansyl and PDA is highly sensitive to R_{ad} and L and that FRET can be optimized by controlling R_{ad} and L. We also report the effect of photopolymerization time, atmosphere (air versus argon in which photopolymerization was performed), and thermal treatment on the absorption spectroscopy of PDA liposomes. The liposomes presented in this study can be used for sensors where the receptor-tagged PDA liposomes can interact with ligands present on proteins, enzymes, and cells which will produce changes in emission sensing signal.

2. Background

We now discuss some important concepts on FRET since the present study involves extensive discussion on FRET. In the FRET process the energy is nonradiatively transferred from a donor molecule(s) to an acceptor molecule(s) through dipole–dipole interactions.[7a] FRET usually results in a decrease in the donor emission (and an increase in the acceptor emission if the acceptor is a fluorophore), quenching and depolarization of donor steady-state fluorescence, and shortening of the donor excited-state lifetime.[7a] In general, the k_{ET}–r^{-6} dependence is derived by assuming point donor and acceptor dipoles. For cases involving conjugated polymers and small fluorophores, this dependence is less clear. For example, a recent computation study shows a weaker than usual r^{-6} dependence at short r, but it recovers to r^{-6} dependence at larger r.[7c] On the other hand, the literature has plenty of examples that have utilized k_{ET}–r^{-6} dependence for studies involving FRET between conjugated polymer and

small fluorophores.[3c,f,l–o] In the absence of a clear k_{ET}–r dependence, we believe that k_{ET}–r^{-6} dependence is more appropriate in our case. The FRET efficiency, E, is defined as follows[7a]

$$E=R_0^6/(R_0^6+r^6) \tag{1}$$

where R_0 is Forster's radius and defined in eq 2 below[7a]

$$R_0(\text{in Angstroms})=0.211(k^2n^{-4}Q_yJ)^{1/6} \tag{2}$$

which corresponds to a separation distance between donor and acceptor at which FRET efficiency is 50%. Here k^2 is an orientation factor between donor and acceptor molecules and varies between 0 and 4 for orthogonal and collinear donor–acceptor dipole orientations, respectively, Q_y is the quantum yield of the donor, J is the overlap between the donor emission spectrum and the acceptor absorption spectrum, and r is the distance between the donor and acceptor.[7a] The spectral overlap interal function, J, is defined as follows[7a,8]

$$J(\lambda)=\int F(\lambda)\varepsilon(\lambda)\lambda^4\delta\lambda/\int F(\lambda)\delta\lambda \tag{3}$$

which is a quantitative measure of the donor–acceptor spectral overlap over all wavelengths (λ), where $F(\lambda)$ represents the donor emission (normalized dimensionless spectrum) at wavelength λ and $\varepsilon_A(\lambda)$ represents the extinction coefficient of acceptor at λ. When one donor simultaneously interacts with several acceptors brought in close proximity, the above efficiency can be expressed as follows[8]

$$E=\left(nR_0^6/(nR_0^6+r^6)\right) \tag{4}$$

where n is the average number of acceptor molecules interacting with one donor. Here, it is assumed that all the interacting acceptors are equally separated from a central donor. In this case, the presence of several acceptor fluorophores will increase the FRET efficiency from donor to acceptors.

Experimental Section

Materials

10,12-Pentacosadiynoic acid was obtained in >95% purity from GFS Chemicals. All organic solvents for synthesis and purification were purchased from Fisher Scientific and used without further purification. Water used in the preparation of liposomes was purified and deionized using standard procedures.

Synthesis of the Fluorescent Lipid Monomers 1

We synthesized three different monomers in the present studies. All three monomers have the same chemical structure except that the linkers connecting the diacetylene moiety with dansyl are different (Figure 1). The linkers for three monomers are ethylene (**1c**), triethylene glycol (**1b**), and tetraethylene glycol (**1a**) moieties. The dansyl–diacetylenes (monomers **1a**, **1b**, and

1c) were chosen such that they have the same chemical structures to diacetylenic acids (monomer **2**) except for the chemical moieties that connect the carboxylic acid of **2** and the dansyl part. Thus, we expect that monomers **1** and **2** will self-assemble in liposomes such that diacetylene functional groups of **1** and **2** will align with one another and participate in the photopolymerization. Synthesis of **1** was accomplished using a procedure similar to published reports (Figure 1).[6a,9]

Synthesis of 3

To a solution of 10,12-pentacosadiynoic acid (monomer **2**, 0.50 g, 1.35 mmol) in 10 mL of methylene chloride CH_2Cl_2, *N*-hydroxysuccinimide (0.174 g, 1.5 mmol) and 1-(3-dimethylaminopropyl)-3-ethylcarbodiimide hydrochloride (0.299 g, 1.55 mmol) were added at room temperature. The solution was stirred at room temperature for 2 h, and the solvent was evaporated under reduced pressure. The residue was extracted with diethyl ether and water three times. The organic layer was dried with $MgSO_4$ for 0.5 h and filtered, and the solvent was removed by rotary evaporation to give 0.45 g of white solid **3**.

Synthesis of 5

Dansyl chloride (0.40 g, 1.49 mmol) was added dropwise to a solution of **4** (11.12 mmol) (**4a**, α,*ω*-diamino-tetraethylene glycol; **4b**, 2,2′-(ethanedioxy)diethylene amine; **4c**, ethylenediamine) in 50 mL of dry THF followed by triethylamine (0.19 g). After stirring overnight, the solvent was removed by rotary evaporation and the residue subjected to silica gel column chromatography (ethyl acetate:methanol 3:1) to give a highly fluorescent intermediate **5** (0.39 g for **5a**, 0.33 g for **5b**; 0.29 g for **5c**).

Synthesis of 1

To a solution of **3** (0.30 g, 0.6 mmol) in 20 mL of dry CH_2Cl_2 was added a solution of fluorescent intermediate **5** (0.6 mmol) in dry CH_2Cl_2. After stirring overnight at room temperature, the mixture was concentrated by rotary evaporation and the residue subjected to silica gel column chromatography (from ethyl acetate:hexane 2:1 to 10% chloroform–90% methanol) to yield the desired fluorescent monomer **1**.

1a, ^{1}H NMR (300 MHz, $CDCl_3$) δ 0.84 (t, 3H), 1.10–1.32 (m, 26H), 1.34–1.52 (m, 4H), 1.52–1.58 (m, 2H), 2.08 (t,2H), 2.15 (m, 4H), 2.89 (s, 6H), 3.00–3.08 (m, 2H), 3.32–3.58 (m, 14H), 5.75 (b, 1H), 6.35 (b, 1H), 7.19–8.61 (6H). Yield of **1a** ~ 52%.

1b, ^{1}H NMR (300 MHz, $CDCl_3$) δ 0.84 (t, 3H), 1.10–1.32 (m, 26H), 1.34–1.52 (m, 4H), 1.52–1.58 (m, 2H), 2.08 (t,2H), 2.15 (m, 4H), 2.89 (s, 6H), 3.00–3.08 (m, 2H), 3.32–3.58 (m, 10H), 6.35 (b, 1H), 7.19–8.61 (6H). Yield of **1b** ~ 53%.

1c, ^{1}H NMR (300 MHz, $CDCl_3$), δ: 0.84 (t, 3H), 1.10–1.32 (m, 26H), 1.34–1.52 (m, 4H), 1.52–1.58 (m, 2H), 2.08 (t,2H), 2.15 (m, 4H), 2.89 (s, 6H), 3.00–3.08 (m, 2H), 3.28 (m, 2H), 5.5 (b, 1H), 5.85 (b, 1H), 7.19–8.61 (6H). Yield of **1c** ~ 56%.

Liposome Preparation

The liposomes were synthesized according to a published literature procedure.[5k,6a] A desired ratio of mixture containing **1** and **2** was dissolved in chloroform in a round-bottom flask, and the solvent was evaporated completely to yield a thin film of monomers. The film was hydrated with either deionized water or PBS (5 mM, pH 7.4) to make a liposome solution of a desired concentration. The resultant suspension was sonicated at 76 °C for ~15 min. The solution was then passed through a 0.8 μm nylon filter to remove the lipid aggregates and cooled at 4 °C overnight to promote self-assembling of the monomers. The resultant solution was optically clear. The diacetylene monomers were polymerized by irradiation with 254 nm of UV

irradiation for ~2–5 min using a Pen Ray UV source (4.5 mW/cm^2) in either air or argon atmosphere. Photodegradation of dansyl was found to be minimal (<10%). The resulting blue liposome solution was stored in the dark at 4 °C. In our investigations the molar ratio of diacetylene acids and dansyl-tagged diacetylene is extremely small (ranges from 200 to 10 000), and we expect the affect of the dansyl group on diacetylene polymerization should be minimal. Our UV–vis analysis did not show any significant differences in the diacetylene polymerization for different concentrations of dansyl in the liposome mixtures. Furthermore, the dialysis data on liposomes using a membrane with M_w cutoff of 10 000 against deionized water indicated that >95% of **1** remains incorporated in the liposomes after polymerization.

Optical Spectroscopy Measurements

UV absorption spectra of all the samples were recorded with a Perkin-Elmer Lambda 25 UV/vis spectrophotometer. The emission spectra were measured with a Photon Technology International spectrofluorometer. For all emission spectra, the excitation wavelength was set at 337 nm and the slit widths (excitation and emission) were 6–8 nm.

To investigate the local environment in which the dansyl fluorophores reside in the liposomes, steady-state fluorescence anisotropy (FA) measurements were carried out using a Photon Technology International spectrofluorometer interfaced with a Peltier cell and fitted with thin film polarizers. FA is defined in eq 5, [7a,10]

$$\mathrm{FA}=(I_v - I_h)/(I_v+2I_h) \quad (5)$$

where I_v and I_h are the vertically polarized and horizontally polarized fluorescence intensities, respectively. All samples were excited at 337 nm, and the polarized emissions were detected at wavelengths of 464 and 560 nm, respectively. The contribution of light scattering to fluorescence intensity was confirmed to be less than 5%. The anisotropy values were corrected for FRET contribution to calculated anisotropy (see below and Supporting Information).[7b] The temperature was gradually increased from 298 to 370 K and maintained at a desired temperature for 10 min before fluorescence measurements were taken at that temperature. The reported anisotropy values are an average of five independent measurements. The contribution of direct excitation to total PDA emission at 560 nm peak is extremely low.[6a]

Fourier-Transform Infrared (FTIR) Measurements

External reflection–absorption FTIR spectra was performed on liposome films coated on gold substrates using a Nicolet Nexus 670 FT-IR fitted with a nitrogen-cooled MCT-B detector and a Velma II variable-angle specular-reflectance accessory operating at a beam incidence angle of 80° with respect to surface normal. The samples were averaged at 1000 scans at 2 cm^{-1} against a background of bare gold substrate. The spectrometer was purged continuously with dry nitrogen gas to minimize water vapor in the sample.

Results and Discussions

PDA is known for chromatic transition when stress is applied to it.[5h–k,6] Following application of stress on the conjugated ene–yne backbone, PDA-based systems exhibit blue to red chromatic transition.[5h–l,m,6] The applied stress reduces the effective conjugated length of the PDA backbone chains and effectively shifts the electronic absorption band to shorter wavelengths.[5k,6a]

Recently, we demonstrated a dansyl–PDA liposome system where dansyl fluorophores were donors and PDA was the energy acceptor.[6a] We showed that the energy transfer efficiency

from dansyl to PDA was high following heating of the PDA liposome system. We attributed the acceptor emission amplification due to changes in J and donor Q_y after thermal treatment of the liposome solution. In this paper, we investigate the effect of polymerization time and environment on the electronic absorption spectrum of the liposomes. We demonstrate here that the FRET efficiency is highly dependent on both R_{ad} and L. A model is also proposed to qualitatively explain the effect of L on FRET between donors and acceptors.

A. Electronic Absorption Spectroscopy of PDA Liposomes

Figure 2A presents a schematic presentation of polymerized liposomes which were composed of monomers **1** and **2** ($[\text{monomer}]_{total}$ = 1 mM). The average particle size was between 50 and 150 nm.[6a]

A.1. Effect of Polymerization Time and Polymerization Environment—The rate of PDA polymerization under two different atmospheres (argon and air) was studied by measuring the absorption peak intensity of PDA liposome solution (Figure 3A). The blue PDA (liposome solution at 298 K) shows a very broad peak with λ_{ab} at ~640 nm and a less intense shoulder at ~590 nm. These peaks are attributed to 0–0′ and 0–n′ electronic π–π* transitions, respectively, of the conjugated polymer backbone.[12] The shape of the electronic absorption spectra remained the same (Figure 1S, Supporting Information) without significant broadening of these two absorption peaks for both air- and argon-polymerized liposomes. This suggested that the number of polymer chains (with an effective conjugation length equivalent to an energy difference of 550–630 nm) increased with polymerization time. The rate of PDA polymerization in argon atmosphere was found to be ~7 times faster than that performed in the air atmosphere (Figure 3A). This significant difference in the polymerization rate is attributed to the presence of oxygen molecules in air which can affect the growing PDA chains.[11] Due to extremely fast PDA polymerization in the inert argon atmosphere, all liposomes used in these studies were prepared in the air atmosphere (polymerization time ≈ 2–5 min). Interestingly, polymerization performed in argon also showed slightly red shifted electronic absorption peak maxima (λ_{ab}) at 648 (for blue phase) and 556 nm (for red phase) compared to λ_{ab} at 640 and 540 nm, respectively, for air-polymerized PDA liposomes (Figure 3A). It is not entirely clear at this point why liposomes polymerized in argon atmosphere showed slightly longer λ_{ab} than those polymerized in air. In general, the growing PDA chains are thought to be either bicarbene or biradical in nature.[11c] It is suggested that the biradical form of the propagating chains is more stable when the degree of conjugation ≤ 4, and the bicarbene form is more stable for longer conjugated PDA chains.[11c] It is, however, not known if the singlet or triplet excited state of bicarbene is involved in the growing polymer chains. In any case, it is possible that both biradical and bicarbene (in fact, bicarbene in the triple excited state will be of radical form) polymer chains can be affected by the presence of oxygen solution. Thus, the presence of oxygen in solution may result in a shortening of the conjugated polymer chains and can result in a slight blue shift in λ_{ab}. From these studies we found that not only was polymerization in argon much faster compared to those in the air atmosphere but they also contained slightly longer effective conjugation length polymer chains.

Figure 3B shows the UV–vis spectra of air-polymerized PDA liposome solution heated to different temperatures. The spectra were taken after the solution was equilibrated for 10 min at a desired temperature. As the temperature of the solution was increased, the peaks centered at ~640 and ~590 nm were decreased in intensity. The intensities of two new peaks centered at ~540 and ~490 nm were observed to increase with temperature (Figure 3B). The blue- to red-phase shift is attributed to decrease in the effective conjugation length of PDA backbone that results in an increase in the energy level of π–π* transitions. We also observed an isosbestic point at 549 nm (Figure 3B) for polymerized liposomes when the solution was heated. The isosbestic point clearly indicates that there are two phases (blue and red) present in the solution

at elevated temperature and that the blue phase converted into red phase without any intermediate phase after thermal treatment of the solution.[13] These thermochromatic changes were irreversible because the red PDA phase is thermodynamically more stable than the blue PDA phase. It is at present, however, not clear if both blue and red PDA phases are present on the same chain or on different PDA chains.

B. IR Spectroscopy on Liposomes

We performed IR spectroscopic analysis to investigate organization of the alkyl portion in the PDA. IR spectroscopy has been used extensively for probing the conformation of self-assembled layers (SAMs) on surfaces, PDA films, and liposomes.[6e,16,17a,b] Previously, using FTIR studies on pH-induced chromic shifts in the PDA materials it was shown that the color change is due to changes in headgroup Hvbonding and its geometry.[6e]

The symmetric (ν_s) and asymmetric (ν_{as}) stretching of *trans*-CH_2 bands in the crystalline alkane are known to exist at 2848 and 2915 cm^{-1}, whereas symmetric and asymmetric bands in liquid *n*-alkane (which contains *gauche*-CH_2) appear at 2856 and 2924 cm^{-1}.[16,17a,b] In our experiments the symmetric and asymmetric CH_2 stretching bands of the alkyl side chains in the liposomes at 298 K (blue phase) were observed at 2849 and 2921 cm^{-1}, respectively. This suggested that the alkyl side chains in the liposomes are somewhat less packed and may contain some gauche configurations. The IR spectrum of the liposomes in the red PDA form ($\nu_s \approx 2850$ cm^{-1} and $\nu_{as} \approx 2921$ cm^{-1}) also indicated less than crystalline-like alkyl side chain packing in the liposomes (Figure 4S, Supporting Information). Furthermore, we also observed a slight increase in the bandwidths of CH stretching peaks after thermal treatment of the solution, which is consistent with less organized packing of the alkyl part in the liposomes.[17c,d] In fact, insertion of EG and dansyl in the bilayers after heating the solution is attributed to less ordering of the alkyl chains in the bilayers. This is consistent with steady-state emission and fluorescence anisotropy measurements (see below).

C. Emission Spectra of Dansyl-Tagged Liposomes

The steady-state emission spectroscopy of dansyl was found to be very valuable to obtain important information on the FRET between dansyl and PDA and on local bilayers environment. The dansyl emission maxima (λ_{em}), full-width at half-maxima (fwhm), and quantum yield (Q_y) are highly sensitive to its local environment in the liposomes, and the solvent-sensitive dansyl emission provides useful information on structure and polarity of the local bilayer environment.[14] For example, with an increase in the polarity of a solvent in which dansyl probes reside we observed that the dansyl Q_y decreased, λ_{em} red shifted to longer wavelengths, and the emission peak broadened (i.e., fwhm of dansyl emission increased). Table 1 provides Q_y, λ_{em}, and fwhm characteristics of dansyl fluorophore **5a** (with chemical structure similar to **1a**, Figure 2S, Supporting Information) in solvents of varying polarities.

Figure 4 shows a typical emission spectra of dansyl-tagged PDA liposomes at different temperatures with $R_{ad,\mathbf{1a}} = 10\,000$ (R_{ad} denotes the ratio of diacetylenic acid (**2**) to dansyl-tagged diacetylene (**1a**) monomers, and **1a** denotes that the donor is **1a**). It is well known that the blue PDA form is nonemissive due to an extremely short excited state lifetime regardless of the presence or absence of energy transfer processes. At $T = 298$ K, the emission spectrum of the liposome solution at 298 K showed an extremely broad and featureless emission peak (λ_{em} at 459 nm and fwhm $\approx$ 105 nm, Figure 4). The location of the dansyl fluorophores in the bilayers is known to vary depending on different factors such as the polarity and viscosity of the local microenvironment and the length of the linking groups that join dansyl with the alkyl portion of the lipid.[15] It is reported that the polar dansyl fluorophores were present at a shallow location near the polar region of the bilayer when the dansyl probes were attached to phospholipids, whereas two different populations (polar and highly hydrophobic part of the

bilayer) were observed when it is attached to dialkylated-C_{16} hydrophobic chains.[15] The presence of a dansyl fluorophore population in a microenvironment of different polarity will increase fwhm because of its polarity-sensitive emission. In our case, the dansyl fluorophores appeared to be present in a range of micropolarities within less organized bilayers of the liposomes (see FTIR below). This is consistent with the steady-state broad and featureless emission spectrum of the liposome solution for dansyl donors **1b** (λ_{ex} = 337 nm; Table 1 and Figure 3S, Supporting Information). With a rise in solution temperature the intensity of broad dansyl emission peak centered at 459 nm decreased and there was a concomitant increase in the PDA emission peak centered at 560 nm. The latter peak is due to PDA emission following FRET from dansyl to PDA.[6a] In our previous studies we observed two PDA emission peaks at 560 and 610 nm.[6a] However, in the present case we did not observe a peak at 610 nm in our emission spectrum. We believe that this peak is buried under a much more intense emission peak at 560 nm which has an unsymmtric peak shape, probably due to the presence of a less intense peak at 610 nm.

In our studies the dansyl fluorophores were attached to conjugated polymer main chains in the liposomes through either ethylene oxide oligomers (**1a** and **1b**) or ethylene (**1c**) linkers. These linkers (**1a** and **1b**) are flexible, water soluble, and have sufficient mobility to insert themselves into the bilayer at various depths. The mechanism between water and polyethylene glycol (PEG) or oligoethylene glycol (OEG) involves formation of hydrogen bonds between water molecules and oxygen atoms of OEG or PEG. When heated these bonds will be broken, which will cause a decrease in the OEG/PEG solubility.[18] In our case the increase in the solution temperature has four major effects on the dansyl emission. First, the solubility of EG linking units was decreased, and this resulted in insertion of EG portions and dansyl of **1a** and **1b** into the bilayer to reduce the free energy of the system. This is reflected in a more featured emission spectrum from a featureless emission spectrum and increased FA of the dansyl (vide infra) after heating of liposome solution. Second, migration of some dansyl fluorophores to a hydrophobic environment in the bilayers led to increased dansyl Q_y (2–7 times depending upon local polarity in which the dansyl resided)[19] and J values, which increased FRET from dansyl donors present in the hydrophobic region to PDA acceptors. Third, the conformational changes in the bilayer structure of the liposomes upon heating the solution can affect the local dielectric constant of the bilayer and the solubility of both EG and dansyl molecules. Fourth, insertion of the EG and dansyl also resulted in increased stress on the PDA backbone, which significantly increased Q_y of PDA and hence a PDA emission peak centered at 560 nm.

Interestingly, there was large a drop in the dansyl emission peak in 400–500 nm region (this emission is from the dansyl population present in the hydrophobic environment) and almost little or no decrease in the 500–540 nm peak intensity (emission peak resulting from dansyl population present in the hydrophilic environment). We believe that this emission characteristic is related to respective environmental donor Q_y dependence on E (eq 2). Since E is linearly related to dansyl Q_y (eq 2), which was much higher for dansyl probes present in the hydrophobic environment than those present in the hydrophilic environment, E was also larger from the dansyl population present in the hydrophobic region.

D. Fluorescence Anisotropy Measurements of Liposomes

We performed steady-state FA experiments to obtain useful information on the emission depolarization of dansyl. There are two opposite factors that affect dansyl FA in our system: The dansyl insertion in the bilayer will increase FA because it will experience reduced rotational freedom and increased bilayer viscosity. On the other hand, FRET will have a diminishing effect on FA because FRET is an additional angular pathway displacement of the emission oscillator.[7a] The steady-state FA for liposome samples composed of **1a** and **2** (R_{ad} = 1000 and $[monomer]_{total}$ = 1 mM) was 0.216 ± 0.002 and 0.162 ± 0.002 at 298 and 328 K,

respectively, for the dansyl emission peak at 459 nm. We estimated the anisotropy values for dansyl probes in nonanoic acid (a solvent of similar viscosity to that of the alkyl portion of our bilayer liposomes where dansyl resides) to be ~0.018 and 0.0014 at 298 and 328 K (correction due to FRET was incorporated in the calculated FA values, see Supporting Information). The observed experimental steady-state FA values of dansyl in our liposomes are significantly larger than those calculated values in a comparable viscosity solvent. This clearly suggested that the dansyl probes feel a highly viscous microenvironment and that the rotational depolarization of dansyl is restricted in our system.

We also performed FA experiments on unpolymerized diacetylene liposomes at different temperatures to get FA information without involvement of FRET factor in the analysis. We found that heating of the unpolymerized diacetylene liposome solution resulted in some polymerization of diacetylene which will again have a FRET component in FA analysis. Therefore, as a control experiment we synthesized nonpolymerized liposomes composed of 1,2-dimyristoyl-*sn*-glycero-3-phosphocholine (DMPC, 1 mM) and dansyl-tagged diacetylene (**1a**, 1 μM) which has a very small value of expected degree of polymerization (polymerizable monomer is 1 out 1000). A Perrin plot of $(FA)^{-1}$ versus (T/η) does not increase linearly, but we found that $(FA)^{-1}$ is not sensitive to (T/η) (Figure 5S, Supporting Information). This data is consistent with our FA data on polymerizable liposomes and suggests that on heating the solution the dansyl fluorophores feel a viscous bilayer atmosphere. In these calculations we assumed that the dansyl lifetime did not change after thermal treatment of the liposomes. Therefore, FA data presented here should be treated as a qualitative analysis. We are now performing more extensive transient lifetime measurements which will provide more accurate FA analysis of our system.

It is noted that the effect of the dansyl attachment of liposomes on dansyl FA is minimum because the dansyl probes are attached to liposomes through flexible chains (tetraethylene glycol, **1a**) and have sufficient rotational freedom. The estimated rotation correlation time for liposomes of 50–200 nm in diameter in water of viscosity 1 cP at 298 K is 0.14 and 0.13 ms, respectively (see Supporting Information) which is many orders of magnitude higher than the dansyl excited-state lifetime. Thus, for all practical purposes the liposome nanostructures are considered stationary with respect to dansyl probes (rotational correlation time is 0.73 and 0.27 ns at 298 and 328 K, respectively).

E. Effect of Thermal Treatment on FRET between Dansyl and PDA

It has been shown previously that heating of dansyl–PDA liposome solution resulted in efficient FRET from dansyl to PDA.[6a] The decrease in the dansyl emission intensity and concomitant appearance of a new emission peak ~560 nm is due to energy transfer from dansyl to PDA (Figure 4).[6a] As the temperature of the solution increases, there is a significant increase in J (Table 1). Moreover, some of the dansyl migrates deeper into the hydrophobic region of the bilayers after heating, which resulted in a many times increase in dansyl Q_y[7a,19] and many orders of increase in Q_y of PDA.[20] Table 1 shows some estimated FRET parameters for the PDA–dansyl system. The estimated apparent Forster's radius (app-R_0) and FRET efficiency for the dansyl–PDA pair are also reported for the dansyl donors situated in solvents of different dielectric constants (Table 1). For our system, app-R_0 for the dansyl–PDA pair in a solvent is defined as the Forster radius for the dansyl–PDA system when the whole dansyl population is solely present in a solvent equivalent to a solvent with a particular dielectric constant. For example, when all the dansyl population is situated in solvent with a dielectric constant of 2 (equivalent to a dielectric constant of hexane), we estimated that the ΔJ ($=J_{min} - J_{max}$) value increased more than 100% when the solution was heated from 298 (J at 298 K is called J_{min}, minimum spectral overlap function in blue PDA form) to 333 K (J at 298 K is called J_{max}, maximum spectral overlap function in red PDA form). With all other parameters remaining

the same, corresponding app-R_0 values were 1.99 and 2.28 nm for $\varepsilon = 2$ and 1.66 and 2.31 nm for $\varepsilon = 5.5$, respectively. As shown in Table 1,ΔR_0 (=app-R_{max} − app-R_{min}) is minimum for dansyl occupied in the polar environment, but the opposite is true for nonpolar solvents. We would like to emphasize that ΔR_0 is a measure of the change in FRET efficiency following a thermal transition from the blue to red PDA form. From the data in Figure 4 we estimate a FRET efficiency (E) of ~30–40% for $R_{ad,1a} = 10\,000$ using $E = (1 - F_{da}/F_d)$,[7a] where F_{ad} and F_d are donor emission intensities in the presence and absence of acceptors. With the assumption that FRET is only affective by ΔJ and ΔQ_y due to heating of the solution from 298 to 333 K and keeping all other parameters in eq 1 the same, our simple calculation suggests that the FRET efficiency (E) for $R_{ad} = 10\,000$ is ~30–60%, which is within the observed E value of 30%. The large uncertainty in the estimated E values is because ΔJ, Q_y, and ΔR_0 are convoluted over a wide range due to the presence of dansyl probes in different polarity microenvironments in the liposomes.

F. Effect of the Acceptor to Donor Monomer (R_{ad}) Ratio on FRET

We conducted a series of experiments to investigate the effect of R_{ad} on the FRET between dansyl donors and PDA acceptors. R_{ad} strongly affects E; large R_{ad} implies that multiple acceptors can interact with one excited donor, whereas the opposite is true for low R_{ad}. Therefore, studies of the effect of R_{ad} on E provide important information on the FRET for our system. Figure 5 shows R_f dependence on temperature for different R_{ad}. We define $R_f = F_T/F_{298}$ (Figures 5 and 6), where F_T and F_{298} are the emission intensities of the PDA peak ($\lambda_{em} \approx 560$ nm) at temperature T and 298 K, respectively. R_f (PDA emission amplification factor) indicates the amplification of PDA emission as a result of FRET response between dansyl fluorophores and PDA backbone chains. Figure 5 systematically shows R_f versus T for three different R_{ad}. For $T < 328$ K, R_f was similar for three R_{ad} values, presumably due to similar ΔJ values. When $T > 328$ K, the maximum value of R_f (denoted by $R_{f,max}$) was observed to decrease with a decrease in R_{ad}. For example, $R_{f,max} \approx 18$, 10, and 7 for $R_{ad} = 10\,000$, 1000, and 200, respectively. The increase in R_f with larger R_{ad} is consistent with the argument that a larger number of acceptors interacted with an excited donor present within the donor–acceptor Forster's radius, resulting in an increase in FRET from donor to acceptors.

We now present an estimation of effective number of acceptors that are statistically present per each donor in our system. A single diacetylene unit is not an acceptor, but the effective oligomer diacetylene unit (ODA) in the red PDA form that acts as an acceptor is composed of ~20–30 diacetylene monomer units.[21] For $R_{ad} = 10\,000$ (the diacetylene monomer to dansyl ratio is 10 000) and assuming Q_y of dansyl and PDA are 0.30 and 0.01, respectively (dansyl Q_y is 0.06–0.67 depending upon the environment it resides in[19] and Q_y of PDA is ~10^{-4} and 0.02 in the blue and red form, respectively[20]), we estimate an effective R_{ad} between 20 and 30 for liposomes $R_{da} = 10\,000$. That is, statistically ~20–30 ODA units have the opportunity to interact and accept energy from each excited dansyl present in the liposomes. This is feasible considering that the ODA acceptor units are delocalized along two planes (one for the outer layer and another for the inner layer in the liposome, Figure 7). On the other hand, for $R_{ad} = 200$, there we roughly estimated four excited dansyl present for every ODA unit. This leads us to argue that for liposomal systems of $R_{ad} = 200$ and 1000 there is more than one excited dansyl donor present per ODA and that the excited dansyl fluorophores will compete with one another for energy transfer to PDA. Some of the excited donors in the liposomes for $R_{ad} = 200$ and 1000 will relax to their ground state by emitting photons without having their energy transferred to acceptor units. This donor emission has also contributed to an increased fluorescence background (i.e., F_{298}) and decreased R_f value (because F_{298} is the dominator in the R_f equation). Collectively, we believe that the increased interactions between dansyl and PDA through the larger number of acceptors per donor molecule and reduced fluorescence

background contributed to a large PDA emission amplification for larger R_{ad} compared to smaller R_{ad} values.

G. Effect of Linker Chain Length (*L*)

FRET efficiency is highly dependent on donor–acceptor interdistance, *r* (eq 1). According to eq 1, with all parameters being the same, an increase in *r* would exponentially decrease *E*. Therefore, investigations involving a linker chain length on *E* are crucial for optimization of FRET between the dansyl and PDA system.

We performed a detailed study to investigate the effect of the chain linker length (*L*) on FRET between dansyl and PDA. The chain linker connects dansyl and diacetylene monomers. We designed dansyl-tagged diacetylene monomers **1a**, **1b**, and **1c** to change *L* systematically for investigating its effect on the energy transfer from dansyl to PDA. *L* is tetraethylene glycol and triethylene glycol for **1a** and **1b**, respectively, and they were longer, more flexible, and have higher solubility than for **1c** (which is ethylene, Figure 1). Figure 6 shows the relationship between R_f and *T* for three different linkers: **1a**, **1b**, and **1c** at constant R_{ad}. For thermal treatment of the liposome solutions below 318 K, R_f is almost the same for all three linkers at a given R_{ad} but R_f values were larger for liposomes composed with longer linkers **1a** and **1b** than those containing **1c** for the same R_{ad} at $T > 328$ K.

Figure 7 schematically shows a proposed model to explain the observed phenomenon regarding the affect of the linker length on energy transfer in our liposomal system. In Figure 7A the blue PDA liposomes are composed of **1c** and **2**. The dotted and solid lines represent the inner and outer PDA backbone chains of the bilayer, respectively. We propose that the dansyl probes, **1c**, are located closer to the bilayer–water interface in the blue PDA form. Heating the solution resulted in an increase in *J* but without significant changes in either *r* or dansyl Q_y (Figure 7B) since **1c** is relatively short and less flexible and the donors were located closer to the bilayer–water interface. On the other hand, for liposomes composed of **2** and **1a** (or **1b**), the solubility of the linking chain EG in water decreases when heating the liposomes[17] (Figures 7C and 7D). Moreover, heating of the liposomes may also result in disordering of the bilayer, which may affect the local dielectric constant of the bilayer and hence the solubility of the dansyl donors and EG in the bilayer. After heating the solution we propose that the flexible and longer EG linkers **1a** and **1b** bent and some of the dansyl were inserted into the hydrophobic layer of the liposomes (Figure 7D). Inclusion of dansyl into bilayers at different depths is also supported by our high dansyl FA and very broad steady-state emission spectra. Dansyl insertion into bilayers had three major affects on donor–acceptor pairs present in solution. First, after insertion of dansyl fluorophores in the bilayers, the excited dansyl for **1a** and **1b** are much closer to the PDA chains than that of **1c** probes. They can interact with multiple PDA chains present in the two layers of the liposomes. This is depicted in the proposed model in Figure 7D in which after thermal treatment (at $T > 328$ K) a larger number of PDA chains are shown to interact with dansyl for **1a** and **1b** than for **1c**. Second, dansyl Q_y after insertion into the bilayers is significantly increased (>2–7 times), which in turn resulted in an increase in *E* (eq 2). Third, insertion of dansyl into the bilayers can further increase the stress onto PDA chains, which would further increase PDA Q_y[5h–l,m,6a] and hence PDA emission. Taking all these factors into account, a higher *E* and lower background signal were observed for liposomes synthesized with longer linkers **1a** and **1b** than those synthesized with shorter linker **1c**.

Finally, we would like to comment on the advantage of using the FRET process over direct excitation of PDA. As discussed in the text, the emission of PDA is dependent on the red phase PDA fraction present in the polymer since Q_y of blue phase PDA is extremely small and does not contribute to the overall emission of PDA. Figure 8 shows the ratio (I_{FRET}/I_{Direct}) as a function of concentration of **1a** monomer in the liposome (at 70°C). Here, I_{FRET} represents the emission intensity of the 560 nm PDA peak following FRET from dansyl to PDA (λ_{ex} = 337

nm) and I_{Direct} represents the emission intensity of the 560 nm peak with direct excitation (λ_{ex} = 470 nm). In all experiments the total concentration of **1a** and **2** is 1 mM. Higher I_{FRET}/I_{Direct} means that the emission intensity of the 560 nm peak from the FRET process is much larger than that from the direct excitation process. We observed that the I_{FRET}/I_{Direct} ratio is highly dependent on [**1a**]. For example, the I_{FRET}/I_{Direct} ratio is ~0.6 for [**1a**] = 1 μM but increases drastically to ~18 for [**1a**] = 200 μM in the liposomes. These experiments clearly suggest that there is much larger emission amplification for the FRET process as compared to direct excitation. We will report in the future protein and bacteria sensing based on FRET–PDA sensors which we found are more sensitive than those based on direct excitation and colorimetric sensors.[22]

Conclusions

We investigated the photophysical and FRET properties for photopolymerized liposomes composed with diacetylenic acid and dansyl-tagged diacetylene monomers. Photopolymerization of diacetylene monomers in argon was ~7 times faster than in air. Thermal treatment of the dansyl–PDA solution showed an isosbestic point at 549 nm, which suggested the coexistence of blue and red PDA phases in solution during thermo-chromatic transition. FRET efficiency was found to depend upon the acceptor to donor ratio (R_{ad}) and the chemical linker that connected the dansyl with the diacetylene moiety. For R_{ad} = 10 000, PDA emission intensity amplified more than 18 times after heating the liposome solution from room temperature to 333 K; however, the increase in PDA emission intensity for R_{ad} = 200 and 1000 was only ~7 and 10 times, respectively. The emission amplification for higher R_{ad} was attributed to interactions of multiple acceptor units with a single excited dansyl probe present within R_0, which resulted in a high FRET efficiency and a lower fluorescence background. On the other hand, in the case of liposomes composed with a low R_{ad} value a reduced FRET efficiency and increased background emission was found. This is because multiple excited donors compete for energy transfer to limited available acceptors. We also proposed a model to explain the observed larger amplification of the acceptor emission for longer linkers than that for shorter linkers following thermal treatment of the solution. We attributed this increased FRET to an increase in Q_y of dansyl and PDA and multiple donor–acceptor interactions.

Supplementary Material

Refer to Web version on PubMed Central for supplementary material.

Acknowledgements

We acknowledge financial funding from the National Institute of Health (GM 8071101 - 01A1) and the National Science Foundation (CMMI 0609349 and CAREER award). S.M. was supported through a NSF-REU award (DMR 0552800). NMR spectrometers were acquired through grants from the NSF (CHE-0421012 and CHE-0619794). We thank Erastus Gatebe for performing FTIR experiments, Profs. Dan Dyer and Ling Zang for use of the FTIR spectrometer and fluorometer, respectively. Stimulating discussions with Profs. Gary Blanchard and Matthew McCarroll are also acknowledged.

References and Notes

1. Skotheim, TA.; Reynolds, J., editors. Handbook of Conducting Polymers. Vol. 3. CRC; Boca Raton, FL: 2007.
2. (a) Thomas SW III, Joly GD, Swager TM. Chem Rev 2007;107:1339–1386. [PubMed: 17385926] (b) McQuade DT, Pullen AE, Swager TM. Chem Rev 2000;100:2537–2574. [PubMed: 11749295]
3. (a) Liu B, Bazan GC. PNAS 2005;102:589–593. [PubMed: 15642947] (b) Xu QH, Wang S, Korystov D, Mikhailovsky A, Bazan GC, Moses D, Heeger AJ. PNAS 2005;102:530–535. [PubMed: 15642946] (c) Xu QH, Gaylord BS, Wang S, Bazan GC, Moses D, Heeger AJ. PNAS 2004;101:11634–11639. [PubMed: 15282375] (d) Gaylord BS, Heeger AJ, Bazan GC. PNAS 2002;99:10954–10957. [PubMed:

12167673] (e) Gaylord BS, Massie MR, Feinstein SC, Bazan GC. PNAS 2005;102:34–39. [PubMed: 15618399] (f) Wang S, Gaylord BS, Bazan GC. J Am Chem Soc 2004;126:5446–5451. [PubMed: 15113216] (g) Guenes S, Neugebauer H, Sariciftci NS. Chem Rev 2007;107:1324–1338. [PubMed: 17428026] (h) Scholes GD, Rumbles G. Nat Mater 2006;5:683–696. [PubMed: 16946728] (i) Smela E. Adv Mater 2003;15:481–494. (j) Chen L, McBranch DW, Wang HL, Helgeson R, Wudl F, Whitten DG. PNAS 1999;96:12287–12292. [PubMed: 10535914] (k) Pinto MR, Schanze KS. PNAS 2004;101:7505–7510. [PubMed: 15136727] (l) Pu KY, Fang Z, Liu B. Adv Funct Mater 2008;18:1321–1328. (m) Gan H, Li Y, Liu H, Wang S, Li C, Yuan M, Liu X, Wang C, Jiang L, Zhu D. Biomacromolecules 2007;8:1723–1729. [PubMed: 17458934] (n) Liu B, Bazan GC. J Am Chem Soc 2006;128:1188–1196. [PubMed: 16433535] (o) He F, Tang Y, Wang S, Li Y, Zhu D. J Am Chem Soc 2005;127:12343–12346. [PubMed: 16131213]

4. (a) Leclerc M, Faid K. Adv Mater 1997;9:1087–1094. (b) Aberem MB, Najari A, Ho HA, Gravel JF, Nobert P, Boudreau D, Leclerc M. Adv Mater 2006;18:2703. (c) Najari A, Ho HA, Gravel JF, Nobert P, Boudreau D, Leclerc M. Anal Chem 2006;78:7896–7899. [PubMed: 17105186] (d) Ho HA, Dore K, Boissinot M, Bergeron MG, Tanguay RM, Boudreau D, Leclerc M. J Am Chem Soc 2005;127(36): 12673–12676. [PubMed: 16144416] (e) Faid K, Leclerc M. J Am Chem Soc 1998;120(21):5274–5278. (f) Dufresne G, Bouchard J, Belletete M, Durocher G, Leclerc M. Macromolecules 2000;33(22):8252–8257. (g) Leclerc M. J Polym Sci, Part A: Polym Chem 2001;39:2867–2873. (h) Ho HA, Boissinot M, Bergeron MG, Corbeil G, Doré K, Boudreau D, Leclerc M. Angew Chem, Int Ed 2002;41:1548–1551.
5. (a) Singh A, Thompson RB, Schnur JM. J Am Chem Soc 1986;108(10):2785–2787. (b) Spector MS, Easwaran KRK, Jyothi G, Selinger JV, Singh A, Schnur JM. PNAS 1996;93:12943–12946. [PubMed: 8917523] (c) Georger JH, Singh A, Price RR, Schnur JM, Yager P, Schoen PE. J Am Chem Soc 1987;109:6169–75. (d) Singh A, Herendeen B, Gaber BP, Sheridan JP. Polym Mater Sci Eng 1987;57:283–285. (e) Tieke B, Wegner G. Makromol Chem 1978;179:1639–1642. (f) Albrecht O, Laschewsky A, Ringsdorf H. Macromolecules 1984;17:937–40. (g) Hupfer B, Ringsdorf H. Chem Phys Lipids 1983;33:263–82. [PubMed: 6640813] (h) Charych DH, Nagy JO, Spevak W, Bednarski MD. Science 1993;261:585–588. [PubMed: 8342021] (i) Spevak W, Nagy JO, Charych DH. Adv Mater 1995;7:85–89. (j) Okada SY, Jelinek R, Charych D. Angew Chem, Int Ed 1999;38:655–659. (k) Okada S, Peng S, Spevak W, Charych D. Acc Chem Res 1998;31:229–239. (l) Volinsky R, Gaboriaud F, Berman A, Jelinek R. J Phys Chem B 2002;106:9231–9236. (n) Kolusheva S, Boyer L, Jelinek R. Nat Biotechnol 2000;18:225–227. [PubMed: 10657134] (m) Kolusheva S, Kafri R, Marina K, Jelinek R. J Am Chem Soc 2001;123:417–422. [PubMed: 11456543]
6. (a) Li X, McCarroll M, Kohli P. Langmuir 2006;22:8615–8617. [PubMed: 17014092] (b) Ma G, Cheng Q. Langmuir 2006;22:6743–6745. [PubMed: 16863214] (c) Ma G, Müller AM, Bardeen CJ, Cheng Q. Adv Mater 2006;18:55–60. (d) Pindzola BA, Nguyen AT, Reppy MA. Chem Commun 2006:906–908. (e) Reppy MA, Pindzola BA. Chem Commun 2007:4317–4338.
7. Lakowicz, JR. Principles of Fluorescence Spectroscopy. Vol. 1. Plenum Press; New York: 1983. (b) Matko J, Jenei A, Matyus L, Damjanovich S, Ameloot M. J Photochem Photobiol B, Biol 1993;19:69–73. (c) Wong KF, Bagchi B, Rossky PJ. J Phys Chem A 2004:5752–5763.
8. Clapp AR, Medintz IL, Mauro JM, Fisher BR, Bawendi MG, Mattoussi H. J Am Chem Soc 2004;126:301–310. [PubMed: 14709096]
9. (a) Spevak W, Nagy TO, Charych DH, Schaefer ME, Gilbert JH, Bednarski MD. J Am Chem Soc 1993;115:1146–1147. (b) Ji EK, Ahn DJ, Kim JM. Bull Korean Chem Soc 2003;24:667–670. (c) Reichert A, Nagy JO, Spevak W, Charych D. J Am Chem Soc 1995;117:829–830.
10. (a) Mosmuller EWJ, Pap EHW, Visser AJWG, Engbersen JFJ. Biochim Biophys Acta 1994;1189:45–51. [PubMed: 8305458] (b) Kolusheva S, Shahal T, Jelinek R. J Am Chem Soc 2000;122:776–780.
11. Moad, G.; Solomon, D., editors. The Chemistry of Radical Polymerization. Vol. 2. Elsevier: New York; 2005. Odian, G. Principles of Polymerization. Vol. 3. John Wiley and Sons; New York: 1991. p. 228Chance, RR. Encyclopedia of Polymer Science and Engineering. Mark, HF.; Bikales, NM.; Overberger, ChG; Menges, G.; Kroschwitz, JI., editors. Vol. 4. John Wiley & Sons; New York: 1986. p. 767-779.
12. Volkov VV, Asahi T, Masuhara H, Masuhara A, Kasai H, Oikawa H, Nakanishi H. J Phys Chem B 2004;108:7674–7680.
13. Leclerc M. Adv Mater 1999;11:1491–1498.

14. Slavik, J. Fluorescent Probes in Cellular and Molecular Biology. CRC Press; Boca Raton, FL: 1994. (b) González-Benito J, Aznar A, Baselga J. J Fluoresc 2001;11:307–314.

15. London E. Biochemistry 1998;37:4603–4611. [PubMed: 9521780]

16. Ulman A. Chem Rev 1996;96:1533–1554. [PubMed: 11848802]

17. Weers, JG.; Scheuing, DR.; Scheuing, DR., editors. Fourier Transform Infrared Spectroscopy in Colloid and Interface Science. American Chemical Society; Washington, DC: 1991. p. 95 (b) Kew SJ, Hall EAH. Anal Chem 2006;78:2231–2237. [PubMed: 16579602] (c) Casal HL, Cameron DG, Kelusky EC, Tullock AP. J Chem Phys 1984;81:4322–4327. (d) Casal HL, Cameron DG, Mantsch H. Can J Chem 1983;61:1736–1742.Weast, RC.; Selby, SM.; Hodgman, CD., editors. The dielectric constants (ε) of different solvents were taken from CRC Handbook of Chemistry and Physics. Vol. 46. The Chemical Rubber Co. Publisher; Cleveland, OH: 1969.

18. (a) Bailey FE, Callard RW. J Appl Polym Sci 1959;1:56–62. (b) Ishizone T, Seki A, Hagiwara M, Han S. Macromolecules 2008;41:2963–2967.

19. Bramhall J. Biochemistry 1986;25:3479–3486. [PubMed: 3755359]

20. Olmsted J, Strand M. J Phys Chem 1983;87:4790–4792.

21. Chance, RR.; Washbaugh, WW.; Hupe, DJ. Polydiacetylenes: Synthesis, Structure and Electronic Properties. Bloor, D.; Chance, RR., editors. Martinus Nijhoff Publishers; Dordrecht, The Netherlands: 1985.

22. Li X, Kohli P. J Am Chem Soc. Manuscript in preparation

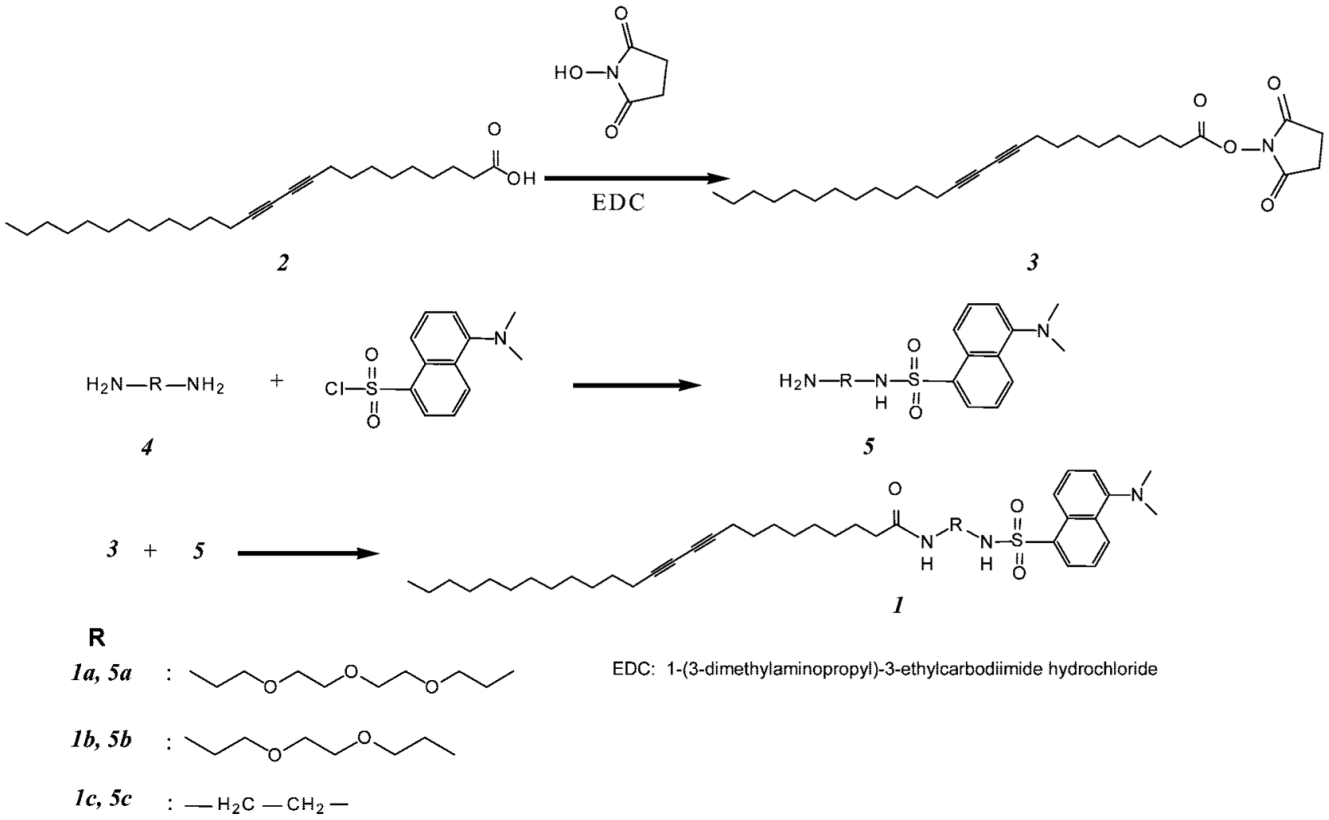

Figure 1.
Synthetic procedures for preparation of the fluorescent diacetylene monomers **1a**, **1b**, and **1c**.

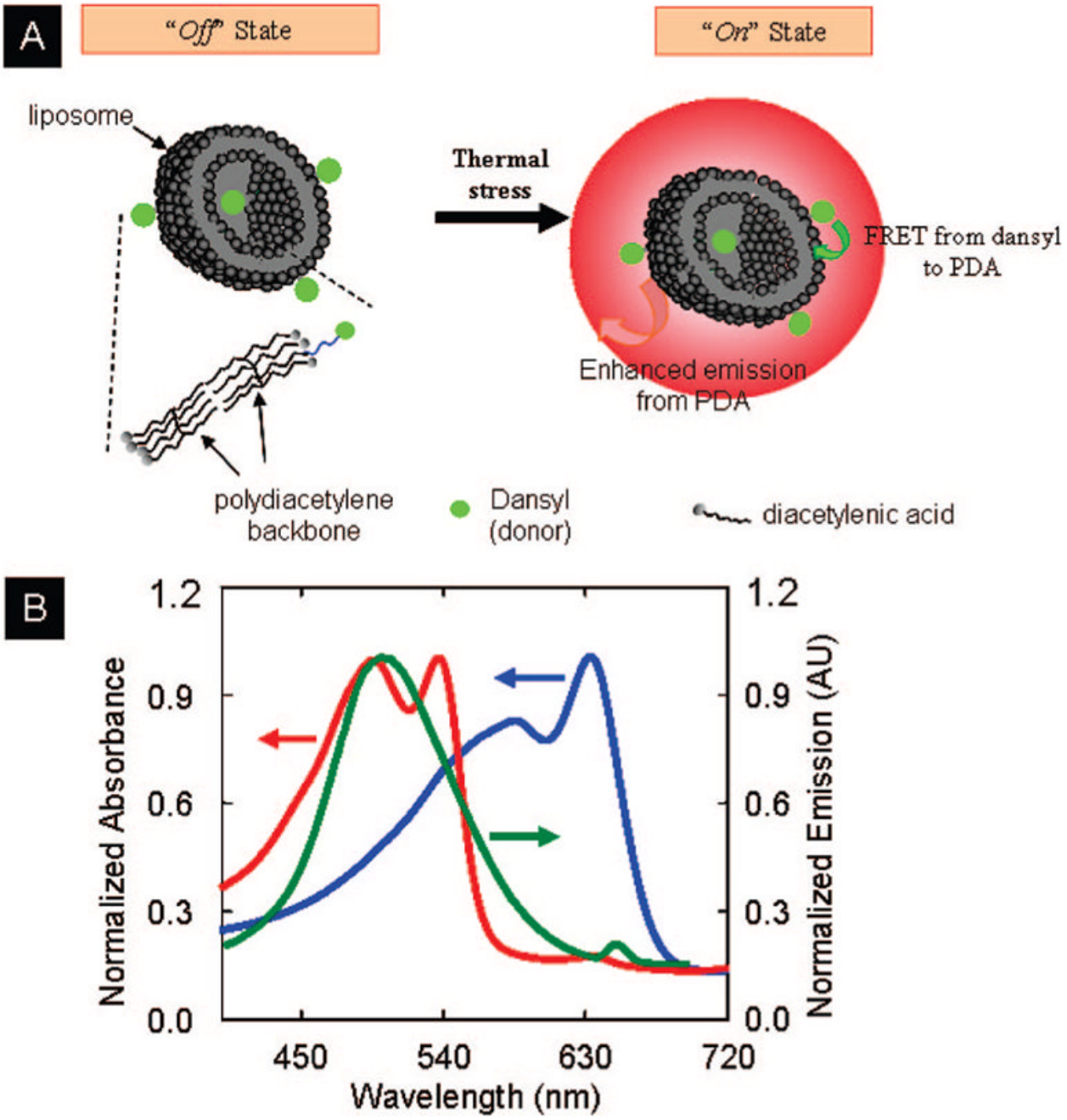

Figure 2.

(A) Schematic representation of a polydiacetylene liposome prepared with a mixture of the fluorescent diacetylene ***1*** and PDA. The "*Off*" state represents when FRET efficiency (*E*) from dansyl to PDA is low, and the "*On*" state represents when *E* is large. (B) Normalized absorption spectra of blue (blue curve) and red forms (red curve) PDA and emission spectrum of dansyl fluorophores (green curve) attached to PDA liposomes (λ_{ex} = 337 nm). The contribution of PDA direct excitation to the total PDA emission for λ_{ex} = 337 nm is extremely small.[6a]

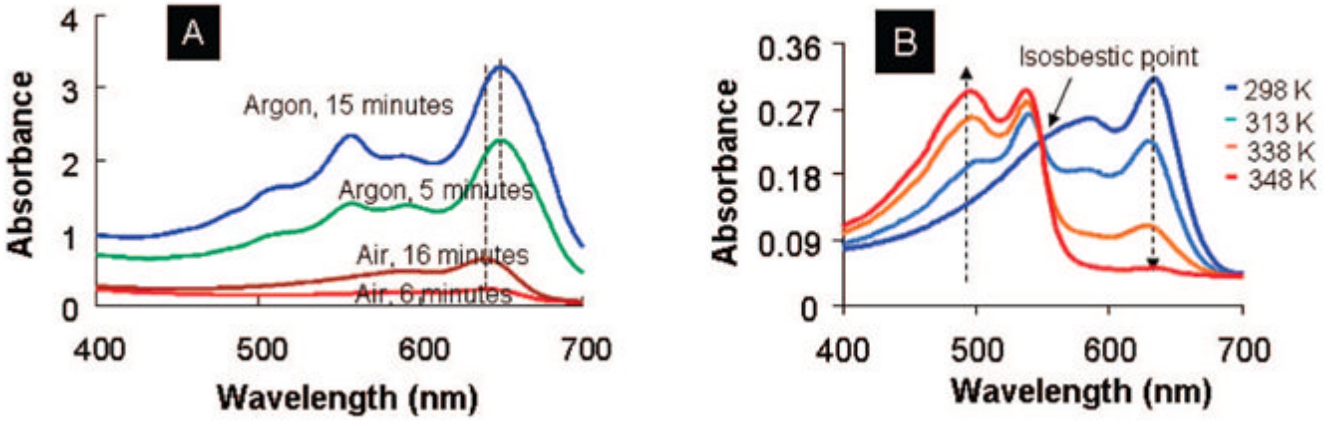

Figure 3.

(A) Comparison of polymerization atmosphere (air versus argon) on the UV–vis absorption spectrum of PDA. Two vertical dotted lines in A show the absorption maxima of blue phase for liposomes polymerized in two different air and argon atmospheres. (B) UV–vis spectra of PDA liposome solution polymerized in air at different temperatures. The peaks centered at 640 and 590 nm of blue phase PDA are attributed to 0–0′ and 0–*n*′ electronic *π*–*π** transitions, respectively. The corresponding peaks in the red phase are centered at 490 and 540 nm, respectively. The arrow marked at 549 nm represents the isosbestic point for two phases (blue and red) in the electronic absorption spectra where the absorptivity of the two PDA phases are same.

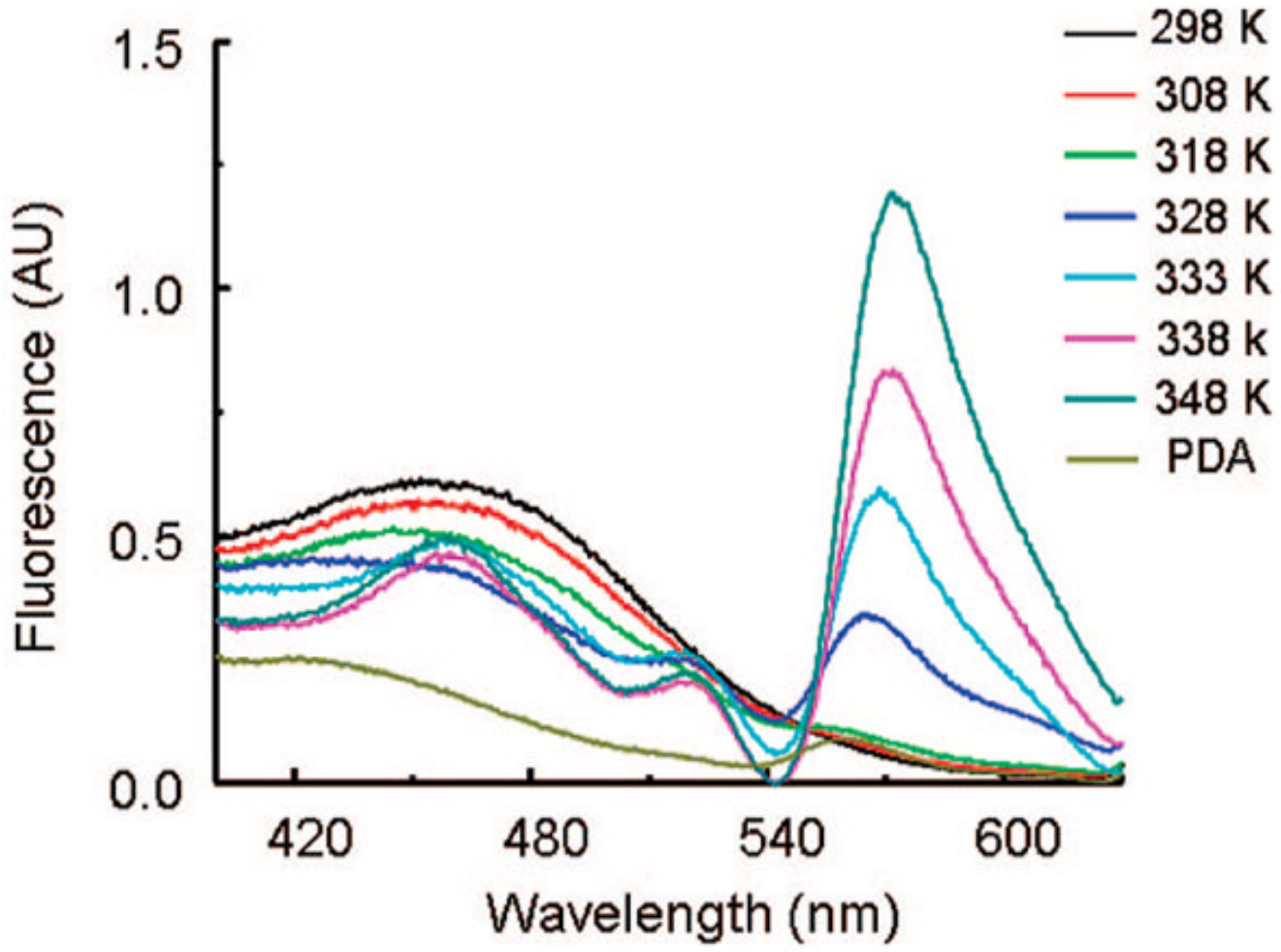

Figure 4.

Emission spectra of dansyl-tagged PDA at different temperatures for $R_{\mathbf{1a}}$ = 1000, subscript **1a** represents that the donor is **1a**. The peaks centered at 459 and 560 nm are, respectively, dansyl emission and PDA emission following FRET (λ_{ex} = 337 nm). The lowest emission intensity spectrum denoted by PDA represents the emission spectrum of 1 mM PDA liposome solution without any dansyl donor molecules in the liposomes (λ_{ex} = 337 nm).

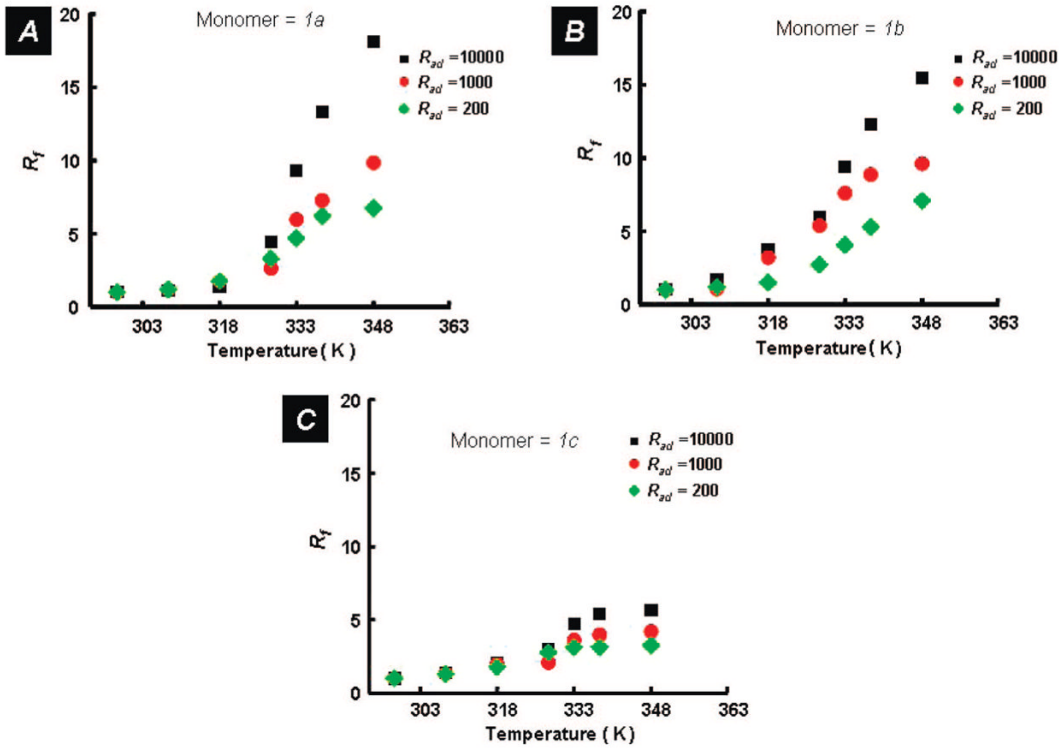

Figure 5.

R_f –temperature dependence for liposomes composed of **2** and (A) **1a**, (B) **1b**, and (C) **1c** with three different R_{ad}. In all cases, $[\text{monomer}]_{total}$ is 1 mM in the final liposome solution. $R_f = F_T/F_{298}$, where F_T and F_{298} are the emission intensities of the PDA peak ($\lambda_{em} \approx 560$ nm) at temperatures T and 298 K, respectively. R_f (PDA emission amplification factor) indicates amplification of PDA emission as a result of FRET response between dansyl fluorophores and PDA backbone chains.

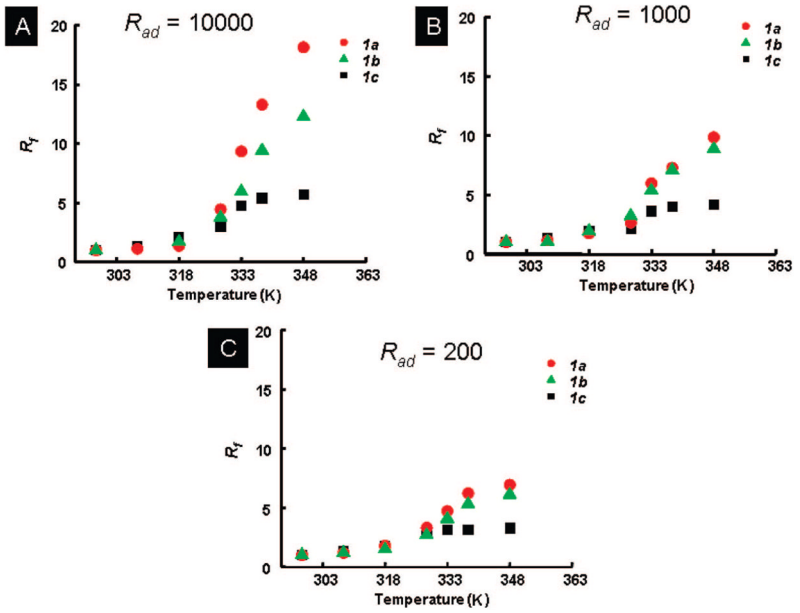

Figure 6.

R_f–temperature dependence for liposomes composed of R_{ad}: (A) 10000, (B) 1000, and (C) 200. In all cases, $[\text{monomer}]_{total}$ is 1 mM in the final liposome solution.

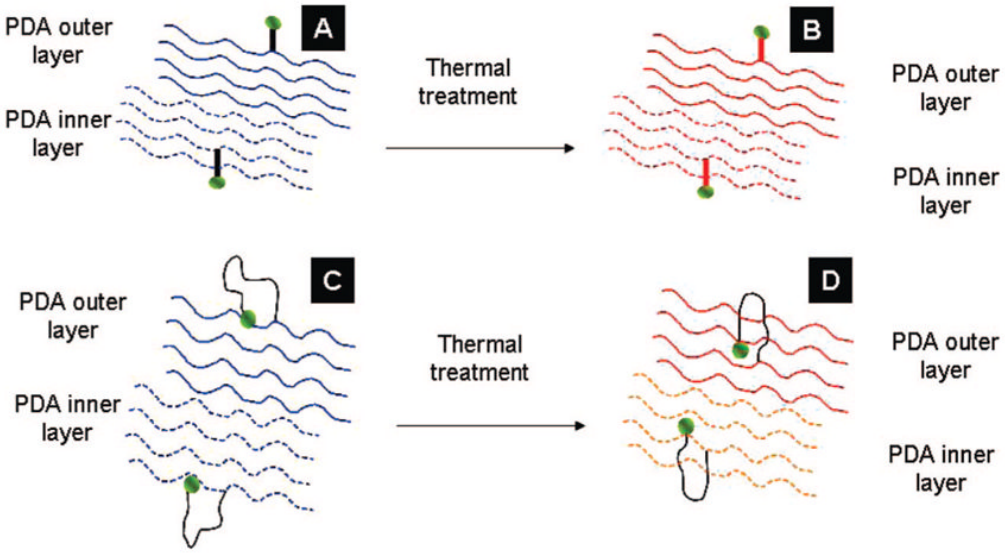

Figure 7.

Proposed FRET model for dansyl–PDA liposomes composed with three different linkers of varying length and rigidity. The schematic presentation of bilayer structures in the liposomes composed of dansyl connected with diacetylene through shorter and less flexible groups (ethylene (**1c**)) and **2** before (A) and after (B) thermal treatment. A similar schematic presentation of bilayer structures of the liposomes composed of donor probes that are connected with diacetylene through longer and flexible groups (triethylene glycol (**1b**) or tetraethylene glycol (**1a**)) and **2** before (C) and after (D) thermal treatment. Note that the probes connected through longer linkers to diacetylene functional groups are depicted inserted deeper into bilayers after heating of the liposome solution.

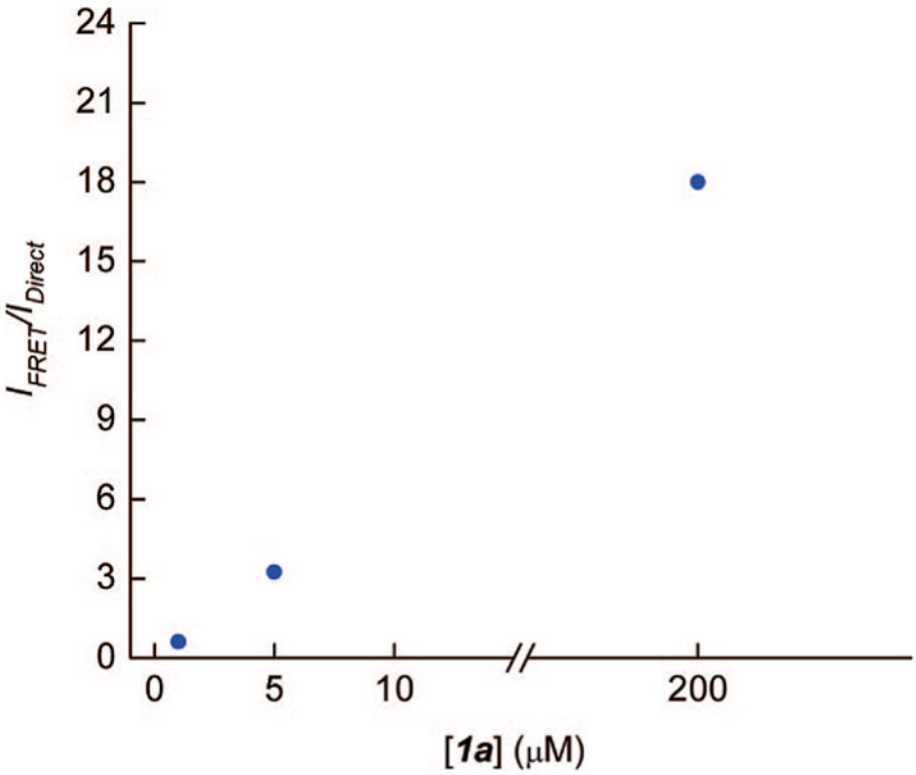

Figure 8.

Ratio I_{FRET}/I_{Direct} as a function of concentration of **1a** monomer in the liposome (at 70 °C). I_{FRET} represents the emission intensity of the 560 nm PDA peak following FRET from dansyl to PDA (λ_{ex} = 337 nm), and I_{Direct} represents the emission intensity of the 560 nm peak following direct excitation (λ_{ex} = 470 nm). The total concentration of **1a** and **2** is 1 mM. Note that I_{FRET}/I_{Direct} is ~0.6 for [**1a**] = 1 μM but increases drastically for higher concentrations of **1a** in the liposomes.

TABLE 1

Emission Characteristics of 5a and Estimated FRET Parameters (J and app-R_0 values) for Dansyl and PDA Pair in Solvents of Different Polarities

Solvent	**polarity (ε)**[i]	**λ_{em} (nm)**	**fwhm (nm)**[h]	**Q_y**[a,19]	**ΔJ (%)**[f]	**app-$R_{0,min}$**[g] **(nm)**	**app-$R_{0,max}$**[g] **(nm)**
Hexane	2	447	70	0.66	127	1.99	2.28
chloroform	5.5	487	72	0.68[b]	616	1.66	2.31
THF	7.5	487	72				
Butanol	17.8	498	86	0.58[c]	63	2.21	2.38
isopropanol	18.3	498	86	0.55[d]			
Ethanol	24	504	91	0.51[e]			
water	78	531	113	0.09	8.2	1.76	1.78

[a] Quantum yield of dansylglycine in a solvent of equivalent dielectric constant given in column 2 of this table (taken from ref [19]).

[b] Solvent of dielectric constant (ε) = 5.2.

[c] Solvent of ε = 16.

[d] Solvent with ε = 20.

[e] Solvent of ε = 25.

[f] $\Delta J = J_{max} - J_{min}$ where J_{max} and J_{min} are the maximum and minimum spectral overlap between emission of dansyl for a given polarity and absorption of PDA liposomes in water at 333 and 298 K, respectively. J_{max} and J_{min} are calculated using eq 2.

[g] app-R_{max} and app-R_{min} are apparent Forster's Radii corresponding to J_{max} and J_{min}.

[h] Measured data in this study (Figure 2S, Supporting Information).

[i] The dielectric constants (ε) of different solvents were taken from ref [17d].